The Basic Effects of Atmosphere–Ocean Thermal Coupling on Midlatitude Variability*

JOSEPH J. BARSUGLI

CIRES, University of Colorado, Boulder, Colorado

DAVID S. BATTISTI

Department of Atmospheric Sciences, University of Washington, Seattle, Washington

(Manuscript received 30 October 1996, in final form 7 May 1997)

ABSTRACT

Starting from the assumption that the atmosphere is the primary source of variability internal to the midlatitude atmosphere–ocean system on intraseasonal to interannual timescales, the authors construct a simple stochastically forced, one-dimensional, linear, coupled energy balance model. The coupled system is then dissected into partially coupled and uncoupled systems in order to quantify the effects of coupling. The simplicity of the model allows for analytic evaluation of many quantities of interest, including power spectra, total variance, lag covariance between atmosphere and ocean, and surface flux spectra. The model predicts that coupling between the atmosphere and ocean in the midlatitudes will enhance the variance in both media and will decrease the energy flux between the atmosphere and the ocean. The model also demonstrates that specification of historical midlatitude sea surface temperature anomalies as a boundary condition for an atmospheric model will not generally lead to a correct simulation of low-frequency atmospheric thermal variance.

This model provides a simple conceptual framework for understanding the basic aspects of midlatitude coupled variability. Given the simplicity of the model, it agrees well with numerical simulations using a two-level atmospheric general circulation model coupled to a slab mixed layer ocean. The simple model results are also qualitatively consistent with the results obtained in several other studies in which investigators coupled realistic atmospheric general circulation models to ocean models of varying complexity. This suggests that the experimental design of an atmospheric model coupled to a mixed layer ocean model would provide a reasonable null hypothesis against which to test for the presence of distinctive decadal variability.

1. Introduction

There is no doubt that the midlatitude atmosphere and oceans form a coupled system, but how important is this coupling on intraseasonal and longer timescales? It is very difficult, if not impossible, to quantify from observations alone the relative importance of the atmosphere and ocean in determining midlatitude low-frequency variability. Any deduction of the relative importance of the atmosphere and ocean will require reference (implicitly or explicitly) to an underlying mathematical or statistical model. At the complex end of the modeling spectrum, studies using realistic atmospheric general circulation models (AGCMs) have been used to examine the impacts of coupling on the natural climate variability in the midlatitudes (e.g., Schneider and Kinter 1994; Manabe and Stouffer 1996; Lau and Nath 1996; Bhatt et al. 1998; Bladé 1997; Nitsche 1996). The methodology used in each of these studies involves the comparison of two integrations of the AGCM. First, the AGCM is integrated using a prescribed sea surface temperature (SST) field (typically, the observed annual cycle). The second integration allows for interactions between the AGCM and either an ocean general circulation model or a surface ocean mixed layer model. Figure 1, reproduced from Manabe and Stouffer (1996), illustrates a large, robust effect seen in each of these studies: compared to the uncoupled integration, the coupled model shows significant enhancement in the variance of the surface air temperature (typically a doubling of the variance due to coupling), with the increased variance arising mainly from changes at low frequencies.

The original motivation for this paper came from the results in Barsugli (1995, henceforth B95), which noted the above effect on surface temperature variance in a numerical model consisting of a two-level atmospheric GCM with zonally symmetric boundary conditions run with perpetual annual-mean insolation, and coupled to a 50-m deep, global mixed layer ocean model. The mod-

* Joint Institute for the Study of the Atmosphere and Ocean Contribution Number 382.

Corresponding author address: Dr. Joseph Barsugli, CIRES, University of Colorado, Campus Box 449, Boulder, CO 80309-0449.
E-mail: jjb@cdc.noaa.gov; david@atmos.washington.edu

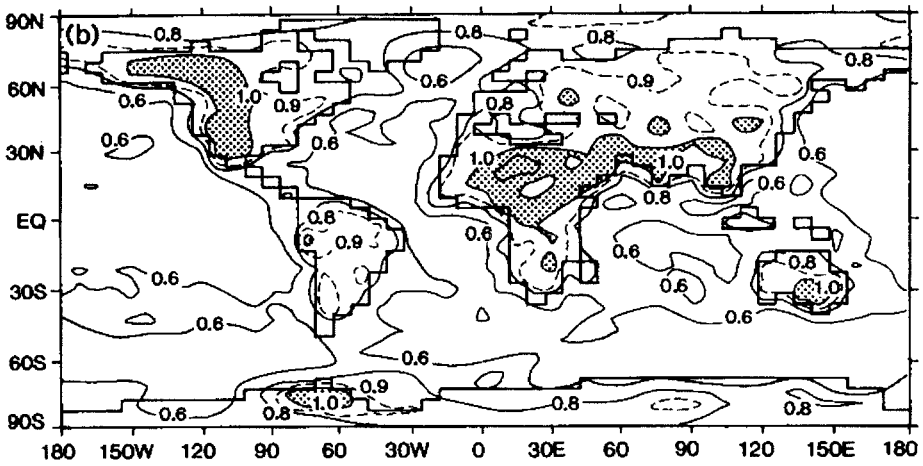

FIG. 1. The ratio of the standard deviation of the 5-yr-mean surface air temperatures from two runs of the GFDL R15 AGCM: (fixed climatological SST)/(coupled to OGCM). [Reproduced from Manabe and Stouffer (1996).]

el was designed to minimize variability in the Tropics so that the variability due to intrinsic midlatitude atmosphere–ocean interactions could be isolated. B95 showed that the strong enhancement of thermal variance (defined as variance in the temperature and associated thermal wind fields) due to coupling occurs mainly for timescales longer than the *e*-folding decay time for a mixed layer temperature anomaly, τ_{ML}, which is approximately 4 months for that numerical model. Here τ_{ML} can be estimated directly from the autocorrelation function for SST anomalies, or by dividing the effective heat capacity of the mixed layer by an empirically derived coefficient relating net surface flux anomalies to SST anomalies. Barsugli showed that coupling reduces the overall variance of surface fluxes seen by the atmosphere, especially for timescales greater than τ_{ML}. Finally, B95 demonstrated that the structures of the atmospheric circulation and surface flux anomalies in the midlatitudes were relatively insensitive to the atmosphere–ocean feedback and argued that the primary effect of coupling was to ''selectively enhance'' the natural low-frequency variability in the midlatitude atmosphere through reduced thermal damping. The atmospheric structures most affected by coupling were the quasi-stationary, equivalent barotropic Rossby waves that dominate the low-frequency variability in this model. Lau and Nath (1996) came to a similar conclusion regarding ''selective enhancement'' using the GFDL AGCM [also confirmed by Bladé (1997) and Nitsche (1996)], as do Bhatt et al. (1998) in their study using the CCM1.

The strength and robustness of the above results from various models lead us to ask: Can we explain the basic effects due to coupling using a much simpler model? This study is directed at answering that question, employing a simple, stochastically forced, coupled atmosphere–ocean model. We start by reviewing the work of Hasselmann (1976) and of Frankignoul and Hasselmann (1977), who considered the simplest stochastic model of SST variability, $dT/dt = F - \lambda T$. Here F represents mixed layer forcing anomalies (with any contribution by feedback removed), T the sea surface temperature anomalies, and λ a feedback parameter. They assumed the power spectrum to F to be white (i.e., flat) for frequencies lower than some high-frequency limit, yielding a red spectrum for T. The SST spectra from their stochastic model was shown to be a reasonable fit to observed SST spectra in the northern Pacific Ocean away from dynamically active regions. The term ''feedback'' as used in the above papers refers primarily to a strong *damping* effect that surface fluxes are presumed to have at low frequencies on an SST anomaly. Unambiguous separation of the ''forcing'' from the feedback is a difficult matter. It is suggested in Frankignoul and Reynolds (1983) that it is best to determine the spectrum of F and the value of λ indirectly by tuning these parameters to fit the power spectrum of observed SST. Nevertheless, they attempt to calculate some ''known'' terms in F directly as well. For illustrative purposes, they then split F and λ into ''known'' and ''unknown'' parts and calculate the lag-correlations between SST and the ''unknown forcing,'' from which the feedback has not been entirely removed. Frankignoul (1985) reviews this and other work on modeling atmosphere–ocean interaction in midlatitudes.

We approach the problem differently, creating a stochastically forced *coupled* model, shown schematically in Fig. 2. Our approach has several advantages. First, as this is a coupled model, *the feedback due to surface heat fluxes will be built into the model.* Second, we will be able to consider feedback due to the atmospheric *dynamical* response to SST anomalies, albeit in a very approximate manner. Third, the coupled stochastic model can be easily configured to represent three commonly

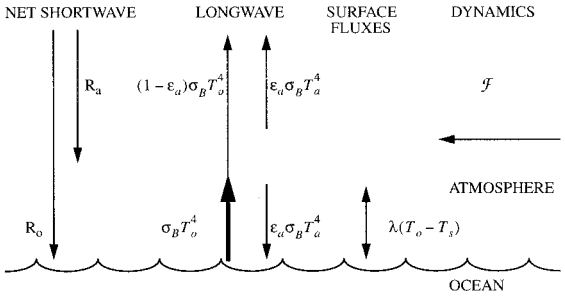

FIG. 2. Diagram of simple energy balance model on which Eqs. (1) and (2) are based. See appendix A for definition of symbols.

used GCM experimental designs: coupled (slab mixed layer), uncoupled (fixed climatological SST), and prescribed time-dependent SST (from observations or a coupled model). Finally, we have identified a plausible candidate for a truly ''white'' forcing of the coupled system in the nonlinear dynamical forcing of the free atmosphere temperature equation. This forcing can be seen in its purest form in an AGCM run with fixed SSTs.[1] We want to emphasize that the *physics* of the surface heat fluxes in Frankignoul and Hasselmann (1977) is the same as in our model, following naturally from a linearization of the bulk formulas for surface fluxes. However, our formulation emphasizes the *role* of surface heat fluxes in reducing the internal damping in the coupled ocean–atmosphere system at low frequencies, allowing for greater thermal variance in both the ocean and atmosphere. We will discuss the role of surface fluxes in coupled and uncoupled models in more detail in sections 3 and 4.

Simple coupled stochastic models are not new. For example, Kim and North (1992) applied a coupled stochastic energy balance model to study various aspects of the coupled atmosphere–mixed layer–deep ocean system, building on earlier work of North et al. (1983). North and Cahalan (1981) briefly compare the expected timescales for scenarios where an AGCM is run with slab mixed layer, fixed SST, or surface energy balance lower boundary conditions. Zubarev and Demchenko (1992) use a coupled stochastic model similar to ours to investigate the relative roles of atmospheric versus oceanic stochastic forcing. Their formalism encompasses our model; however, the parameter values assumed by these authors leads to excessive sensitivity to coupling. Finally, highly idealized, deterministic uncoupled models were used by Schopf (1985), Frankignoul (1985, §4), and Marotzke and Pierce (1997) to investigate the role of the atmospheric response to a SST anomaly. These studies concentrate on the dependence of the decay time of an SST anomaly on the spatial scale of the anomaly. Frankignoul (1985) also considers the quasi-steady coupled case.

The paper is structured as follows. In section 2 we describe and analyze a stochastically forced coupled energy balance model that captures the basic effects of coupling on low-frequency variability. In section 3 we show power spectra of SST, atmospheric temperature and surface fluxes, as well as lagged linear regressions between atmospheric temperature and SST. In section 4 we present a discussion of the salient results from this study along with their implications. In section 4c we summarize results from several recent studies in which coupled, uncoupled, and prescribed SST experiments were performed using full atmospheric GCMs and discuss the results from these studies in light of the expectations from the simple model presented here. Conclusions are presented in section 5.

2. A simple stochastically forced energy balance model of coupled variability

a. Model development

The model we propose to account for the basic effects of coupling between the atmosphere and the ocean in the midlatitudes is displayed schematically in Fig. 2. It is a one-dimensional thermodynamic model for the upper (slab) ocean coupled to a graybody atmosphere. The single spatial dimension represents a typical point in the midlatitudes, although we also interpret the model variables in terms of individual horizontal modes of the atmosphere–ocean system. There is an assumed random forcing associated with the ubiquitous dynamical motions in the midlatitude atmosphere. The equations for this model, linearized about the climatological mean state, are as follows [see appendix A; also cf. Schopf (1985)]:

$$\gamma_a \frac{d\tilde{T}_a}{dt} = -\lambda_{sa}(\tilde{T}_s - \tilde{T}_o) - \lambda_a \tilde{T}_a + \tilde{\mathcal{F}} \qquad (1)$$

$$\gamma_o \frac{d\tilde{T}_o}{dt} = -\lambda_{so}(\tilde{T}_s - \tilde{T}_o) - \lambda_o \tilde{T}_o. \qquad (2)$$

Subscripts ''a'' and ''o'' refer to atmosphere and ocean respectively; $\tilde{T}$ is the anomalous temperature; γ the heat capacity; λ_s the linearized coefficient of combined latent, sensible, and longwave heat flux (values of λ_{sa} and λ_{so} differ only slightly); and λ_a, λ_o the radiative damping of each component to space. Surface heat fluxes are calculated using the surface air temperature $\tilde{T}_s$. The term $\tilde{\mathcal{F}}$ represents the dynamical component of the forcing, which we take to be stochastic.

We assume that the surface air temperature anomaly is linearly related to the free atmosphere temperature

[1] Note that in one example Frankignoul and Hasselmann (1977) use the barotropic vorticity equation to model uncoupled atmospheric wind variability and use meridional velocity anomalies as a proxy for anomalies in air–sea temperature difference. However, they do not consider the role of the atmospheric dynamical response to SST anomalies.

TABLE 1. The standard parameter values as defined in the text and in appendix A.

Parameter	Value	Parameter	Value
γ_a	1×10^7 J m^{-2} K^{-1}	a	1.12
γ_o	2.0×10^8 J m^{-2} K^{-1}	b	0.5
λ_{sa}	23.9 W m^{-2} K^{-1}	c	1
λ_{so}	23.4 W m^{-2} K^{-1}	d	1.08
λ_a	2.8 W m^{-2} K^{-1}	β	20
λ_o	1.9 W m^{-2} K^{-1}	$\lvert N\rvert$	1
λ	20 W m^{-2} K^{-1}	$z \equiv \frac{ad}{\alpha} \equiv \frac{ad}{bc}$	2.42

anomaly, $\tilde{T}_s = c\tilde{T}_a$. We take the Fourier transform ($t \rightarrow \omega$) of Eqs. (1) and (2) and divide through by λ_{sa} to yield

$$i\sigma T_a = -aT_a + T_o + F(\sigma) \tag{3}$$

$$i\beta\sigma T_o = cT_a - dT_o. \tag{4}$$

We have made the following substitutions: $\sigma = \gamma_a\omega/\lambda_{sa}$, $a = \lambda_a/\lambda_{sa} + c$, $d = \lambda_o/\lambda_{so} + 1$, $\beta = (\gamma_o/\gamma_a)(\lambda_{sa}/\lambda_{so})$, and $F = \mathcal{F}/\lambda_{sa}$. A tilde denotes a time-domain variable, and an unadorned variable the corresponding Fourier transform variable. Explicit reference to the independent variables t and σ will be used only for emphasis or to avoid confusion. The derivation of Eqs. (1) and (2) from a more detailed energy balance model is presented in appendix A, where reasonable values of the model parameters are also justified. These parameter values, shown in Table 1, will be referred to as the ''standard parameters'' and are used in the examples to follow.

Equations (3) and (4) as they stand are not suitable for comparing coupled and uncoupled systems because the dynamical forcing term F includes the effects of coupling and will differ between coupled and uncoupled runs. To illustrate this point, we calculate the power spectrum of T_a. From Eq. (3) we have

$$|(i\sigma + a)|^2|T_a|^2 = |F|^2 + |T_o|^2 + FT_o^* + T_oF^*, \tag{5}$$

where * denotes complex conjugation. The term $|T_a|^2$ is the power spectral density for atmospheric temperature, and FT_o^* is the Fourier transform of the lag-covariance function between F and T_o. The lag-covariance terms in Eq. (5) indicate that we must account for the dependence of F on T_o in our theory of the effects of coupling.

In the analysis that follows we will split the dynamical forcing into an SST-forced deterministic part and a purely random part as follows: $F = (b - 1)T_o + N$, where b is a real constant. We have assumed that the dynamical response is proportional to the SST anomaly at the low frequencies of interest. We assume that the power spectrum of N is independent of the coupling to the ocean, hence ''inherent'' to the atmosphere. When substituted into Eq. (3), the total ''thermal'' and ''dynamical'' response becomes bT_o, and we will refer to b as the ''atmospheric response parameter.'' In actuality the temperature response of the free atmosphere to diabatic heating is accomplished largely by dynamical adjustment; therefore we will focus only on the total response in the rest of this paper.

With the above assumptions about the atmospheric response, Eqs. (3) and (4) are in the standard form of a two-variable linear system (with stochastic forcing only in the atmosphere equation)[2]:

$$i\sigma T_a = -aT_a + bT_o + N \tag{6}$$

$$i\beta\sigma T_o = cT_a - dT_o. \tag{7}$$

The coefficients a and d represent damping of the atmosphere and ocean respectively, and the coefficients b and c represent the coupling between atmosphere and ocean. At this point it is useful to define a coupling coefficient

$$\alpha = bc,$$

which represents the feedback due to atmosphere–ocean coupling, and a stability parameter

$$z = ad/\alpha,$$

which results from the competition between this feedback and damping. Note that the atmospheric damping parameter, a, contains a dependence on the parameter c.

b. Methodology

The design of the numerical experiments in B95 will be repeated using the simple model presented in this paper. This design consisted of three model runs as follows.

1) Coupled: The coupled model was run first.
2) Uncoupled: (a) The atmosphere model was run with SST fixed to be the zonal mean of the climatology of the coupled run. (b) The slab mixed layer model was integrated in diagnostic mode, forced with the time history of winds and temperatures from run 2a.
3) MOGA [Midlatitude Ocean, Global Atmosphere, after Lau and Nath (1994)]: (a) The atmosphere model was run with SST prescribed to be the time history of SSTs from the coupled run. (b) The slab mixed layer model was integrated in diagnostic mode, forced with the time history of winds and temperatures from run 3a.

Equations (6) and (7) can be used to model the coupled, uncoupled, and MOGA experiments as follows. The ''coupled'' model (denoted by superscript C) solves Eqs. (6) and (7) as a coupled set:

$$\sigma_a T_a^C = bT_o^C + N^C \tag{8}$$

$$\sigma_o T_o^C = cT_a^C. \tag{9}$$

[2] For illustrative purposes, an even simpler system may be constructed by replacing Eq. (6) with $T_a = M + bT_o$, where M is a stochastic process with a specified power spectrum, perhaps derived from the output of an uncoupled GCM run.

Given N^C, one can solve for T_a^C and T_o^C. We have introduced the abbreviated notation $\sigma_a = (i\sigma + a)$ and $\sigma_o = (i\beta\sigma + d)$. For the ''uncoupled'' system, denoted by superscript U, we get the following set of equations:

$$\sigma_a T_a^U = N^U \tag{10}$$

$$\sigma_o T_o^U = cT_a^U. \tag{11}$$

Equation (10) was obtained by setting $T_o = 0$ in Eq. (6), since SST is fixed at climatological values. Given N^U, one can solve for T_a^U. Equation (11) is the diagnostic equation for a ''slave ocean'' driven by the uncoupled atmosphere, which we solve to get T_o^U. Finally, to model the prescribed SST experiment (MOGA, denoted by superscript M), we set $T_o = T_o^C$ in the atmosphere equation and use the MOGA atmosphere to force a ''slave'' mixed layer ocean, yielding the following equations:

$$\sigma_a T_a^M = N^M + bT_o^C \tag{12}$$

$$\sigma_o T_o^M = cT_a^M. \tag{13}$$

In addition, we assume that N^M and T_o^C are uncorrelated. Recall that the direct effect of the prescribed SST on the dynamical forcing, including any reorganization of the atmospheric eddy fluxes, is accounted for by the dynamical response term $(b - 1)T_o^C$. This latter assumption will simplify the calculation of power spectra for the case of prescribed SST and is, in fact, central to the success of this simple model.

We have assumed that the natural variability of the atmosphere is unaffected by coupling to the surface. Mathematically, N^M, N^U, and N^C should be considered as separate realizations of the same random process, with the same power spectra. The superscripts on N included in Eqs. (8)–(13) only clarify the above assumption and will be dropped for all the following calculations. The models in Eqs. (8)–(13) are formally equivalent to linear Markov processes. The uncoupled system can be cast as one-dimensional Markov processes: T_a^U as a first-order process, and T_o^U as a second-order process. The coupled system can be cast as a two-dimensional, first-order Markov process, and the MOGA system as a four-dimensional, first-order Markov process, subsuming the coupled system. However, we have chosen to keep the models in a form that highlights the physical parallelism between the systems.

The methodology of the coupled, uncoupled, and MOGA experiments as expressed in Eqs. (8)–(13) illuminates the effect of coupling the atmosphere and ocean in the midlatitudes. The results of the uncoupled experiment, along with the diagnostic SST field, serve as the ''uncoupled null hypothesis'' against which we test for the basic effects of thermal coupling. Our analysis of the MOGA experiment has bearing on understanding the role of midlatitude SST anomalies in seasonal climate prediction. In addition, the MOGA experiment aids in the interpretation of the role of the midlatitudes in the simulations done as part of the Atmospheric Model Intercomparison Project (Gates 1992), in which the global historical SST field was specified as a boundary condition for realistic AGCMs. These diagnostic mixed layer model experiments provide a ''common currency'' for comparing the atmospheric variability in the coupled, uncoupled, and MOGA runs in terms of the effect of the atmosphere on SST variability.

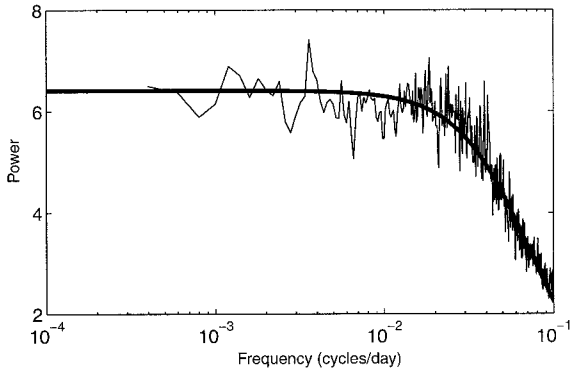

FIG. 3. Power spectrum of 5-day-mean vertical-mean atmospheric potential temperature from a long run of the two-level model of B95 with fixed SSTs (thin line). Spectral estimates are the average estimates from 16 records of 2500 days each, using a Hanning window. No significance is claimed for any individual spectral peak. The thick line is the best-fit stochastic model spectrum from Eq. (16), with damping timescale of 2 days.

c. *Comments on the stochastic forcing and the coupling parameters*

The noise forcing $N(\sigma)$ and the coupling parameters b and c represent the distillation of complicated atmospheric dynamics and deserve further comment. Figure 3, adapted from B95, shows that the low-frequency portion of the spectrum of atmospheric temperature from a long integration of the two-level model is well approximated by Eq. (16), assuming white noise forcing and a total damping timescale of about 2 days. The salient features reproduced are the flat spectrum at low frequencies and the drop-off toward higher frequencies. The damping timescale is about half that of the ''standard parameters,'' with the discrepancy probably due to neglecting the dynamical damping term discussed in appendix A, although the choice of an effective heat capacity of the atmosphere is also an issue. Equation (10) is not meant to be a sophisticated model of atmospheric low-frequency variability but only an approximate representation that we use as a starting point to illustrate the effects of coupling.

We reiterate that nonlinear potential vorticity dynamics is driving the low-frequency variability of the atmosphere. The ''noise'' therefore results from the nonlinearities in the equations of motion, as well as from the representation of a multidimensional system

in terms of one variable. For this simple model, we focus solely on the thermal component of the potential vorticity forcing because numerical experiments lead us to believe that the greatest effect of coupling will be on temperature (and associated thermal wind) variance, which we refer to as ''thermal variance.'' For simplicity, in the analytic calculations presented in sections 3b–d we will assume N to be white noise of unit amplitude.

We have parameterized the atmospheric response to an SST anomaly as bT_o, which includes the linear dynamic and diabatic response as well as the portion of the nonlinear response that can be linearly parameterized in terms of SST. Based on B95 we expect the dynamical portion of the response to act generically as a negative feedback, with atmospheric heat fluxes partially offsetting the diabatic effects of an SST anomaly. That is, we expect that $0 < b < 1$. (Other possibilities are discussed in section 4a.) The simplest measure of b is obtained by solving the time mean of Eq. (12) for the case of a GCM with steady SST anomaly forcing (superscript ''S''):

$$aT_a^S = bT_o^S$$

[cf. Zubarev and Demchenko (1992), with their $\hat{X}_Y$ equivalent to our b, and $\hat{Y}_X = c$]. In a similar vein, one can estimate the atmospheric response from the linear regression of the atmospheric response to time-varying SST anomalies, choosing an appropriate mid-latitude SST anomaly index as the basis for the regression. Barsugli does just that for a two-level idealized atmospheric GCM, and shows that the local free-atmosphere temperature response is roughly 0.5 Kelvin per degree of SST anomaly. Because $a \approx 1$, it is reasonable to choose $b \approx 0.5$ as a bulk measure of the free atmosphere temperature response. A good indication of the effects of the nonlinear dynamical feedback in the two-level model of B95 can be obtained by comparing the linear and nonlinear responses to typical SST anomalies. The linear response to the same SST anomaly is roughly twice that of the nonlinear response and has similar horizontal structure in the region of the largest SST forcing, indicating that the nonlinearity is acting primarily as a damping on the linear response.

The proportionality between T_a and T_s can be estimated from the low-frequency variance of the uncoupled diagnostic ocean, Eq. (11), which is forced by the uncoupled atmosphere:

$$d^2|T_o^U|^2 = c^2|T_a^U|^2.$$

Comparing the low-frequency portion of the spectra of SST and of the vertically integrated potential temperature from the two-level model of B95 indicate an approximate value of $c \approx 0.8$ for that measure of the free atmosphere temperature. For simplicity of interpretation, we will assume $c = 1$ for the standard parameters.

In general, the coupling coefficient α will depend on the vertical structures of the uncoupled atmospheric variability, of the stochastic forcing, and of the diabatic effects associated with coupling, and on how well these project on one another. These dependencies in turn are a function of the horizontal structure of low-frequency variability. In light of this complexity we view α as a characteristic coupling coefficient for the entire coupled system. We have chosen the vertical mean temperature as the appropriate free atmosphere temperature variable because of the dominant role played by equivalent barotropic, quasi-stationary structures in low-frequency variability. Later we shall see how deep and shallow atmospheric modes can be interpreted in terms of varying strengths of this coupling coefficient.

3. Solutions

a. Power spectra in the coupled, uncoupled, and MOGA systems

As noted above, the stochastic model can be used to interpret coupled, uncoupled, and MOGA experiments. The stochastic model allows us to predict how coupling affects variance (power) in the three experiments. In the coupled case (superscript C) we solve the coupled set of Eqs. (8) and (9) for the power spectral densities $P_a^C(\sigma) = |T_a^C|^2$ and $P_o^C(\sigma) = |T_o^C|^2$ as follows:

$$P_a^C = \frac{|\sigma_o|^2|N|^2}{|\sigma_a\sigma_o - \alpha|^2} \tag{14}$$

$$P_o^C = \frac{c^2|N|^2}{|\sigma_a\sigma_o - \alpha|^2}. \tag{15}$$

For the uncoupled (superscript U) case we solve Eq. (10) for the atmospheric power spectrum. The power spectrum for T_o^U, the slave ocean temperature, follows from the diagnostic ocean equation (11). In that case we get for the power spectra:

$$P_a^U = \frac{|N|^2}{|\sigma_a|^2} \tag{16}$$

$$P_o^U = \frac{c^2|N|^2}{|\sigma_a\sigma_o|^2}. \tag{17}$$

For the MOGA case (superscript M), we solve Eq. (12), assuming that N and T_o^C are uncorrelated. Thus, when we calculate the power spectrum of T_a^M the cross-terms between N and T_o^C are zero. As in the uncoupled case, the MOGA atmosphere is used to force a slave mixed layer ocean. The power spectra for the MOGA case are as follows:

$$P_a^M = \frac{|N|^2}{|\sigma_a|^2}\left(1 + \frac{|\alpha|^2}{|\sigma_a\sigma_o - \alpha|^2}\right) \tag{18}$$

$$P_o^M = \frac{c^2|N|^2}{|\sigma_a\sigma_o|^2}\left(1 + \frac{|\alpha|^2}{|\sigma_a\sigma_o - \alpha|^2}\right). \tag{19}$$

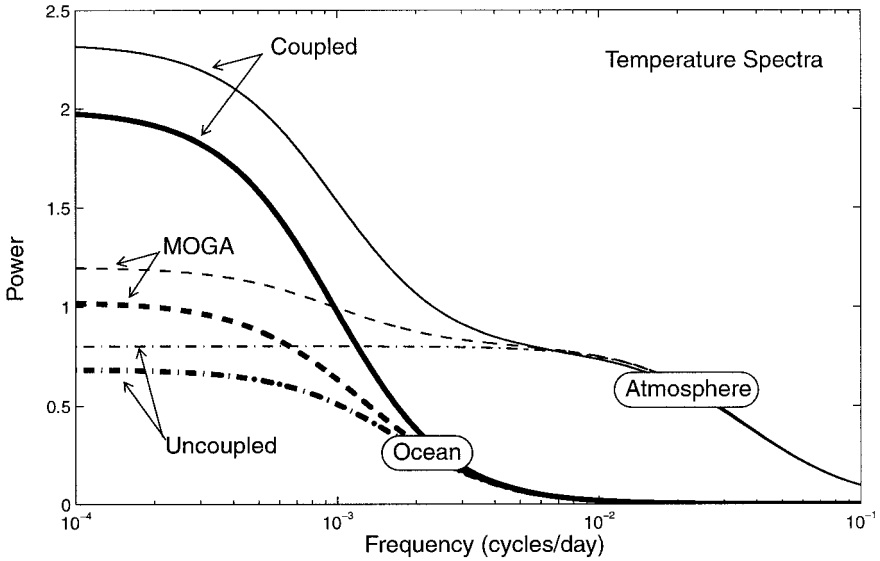

FIG. 4. Power spectra of atmosphere and ocean temperature for the coupled, MOGA, and uncoupled cases. The standard parameters (see Table 1) are used.

Plots of these quantities are shown in Fig. 4 for the standard parameters, with N assumed to be white noise with unit amplitude. Note that the uncoupled atmosphere power is pure ''red noise''—the result of a first-order Markov process with autocorrelation time of a^{-1}, or in dimensional units, $\tau_a = \gamma_a(\lambda_{sa} + \lambda_a)^{-1}$. For the standard parameters $\tau_a \approx 4$ days.

We are now in a position to draw some general conclusions about variance in coupled and uncoupled runs. The MOGA power spectrum for either atmosphere or ocean temperature can be expressed in terms of the respective coupled and uncoupled power spectra as follows:

$$P^M_{a,o} = P^U_{a,o}\left(1 + \frac{|\alpha|^2}{|\sigma_a\sigma_o - \alpha|^2}\right) \tag{20}$$

$$P^M_{a,o} = P^C_{a,o}\frac{|\sigma_a\sigma_o - \alpha|^2 + |\alpha|^2}{|\sigma_a\sigma_o|^2}. \tag{21}$$

At this stage we have not assumed anything about the shape of the spectrum of the forcing term N. We can see that at all frequencies, both the coupled and MOGA runs have more variance than the uncoupled run, at least for reasonable values of α. The comparison of the MOGA and coupled runs is more complicated. For low frequencies, $\beta\sigma^2 < ad$, the coupled variance exceeds the MOGA variance. For higher frequencies, the direct forcing by the SST anomalies exceeds the internal variance. However, due to the long timescales associated with the ocean there is little power at these higher frequencies.

It is instructive to consider the ratios of variance between different systems in the limit as $\sigma \to 0$ (or equivalently, $\omega \to 0$) as follows:

$$\delta^{C,U} = \frac{z^2}{(z-1)^2} \tag{22}$$

$$\delta^{M,U} = 1 + \frac{1}{(z-1)^2} \tag{23}$$

$$\delta^{C,M} = \frac{z^2}{(z-1)^2 + 1}, \tag{24}$$

where $z = ad/\alpha$ as before. We have defined the ratio $\delta^{C,U} = P^C(0)/P^U(0)$, with the other ratios defined analogously, and have dropped the subscripts because these ratios are the same for the atmosphere and ocean variables. (This equality of variance ratios does not necessarily hold in more realistic models, as discussed in section 4a.) The ratio of power at low frequencies depends only on the stability parameter z. A plot of the above power ratios as a function of z is shown in Fig. 5. The standard parameters correspond to $z = 2.42$, and this value is indicated by a vertical line in the plot.

As previously mentioned, z is a stability parameter for the coupled system. For $z > 1$, the coupled system is stable, and the power in the system is maintained by the stochastic forcing. Large values of the stability parameter, $z \gg 1$, correspond to either large damping, large negative atmospheric feedback, or inefficient coupling between the free atmosphere and the surface. In this case the MOGA variance approaches the uncoupled variance, while the coupled variance approaches the uncoupled variance, though much more slowly. In the limit as $z \to 1$, which is off the scale of Fig. 5, the coupled and MOGA variances become equal, and both approach infinity. This limit corresponds to the unrealistic case where positive atmospheric feedback completely counteracts damping. Even in the case where we allow no

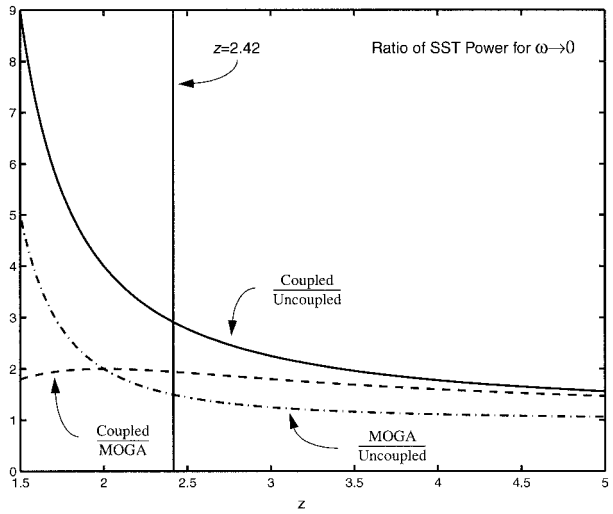

FIG. 5. Ratio of power in SST between the coupled and uncoupled (solid line), coupled and MOGA (dashed line), and MOGA and uncoupled (dash–dot line) cases in the limit as the frequency ω approaches zero. The thick vertical line at $z = 2.42$ indicates the standard parameters.

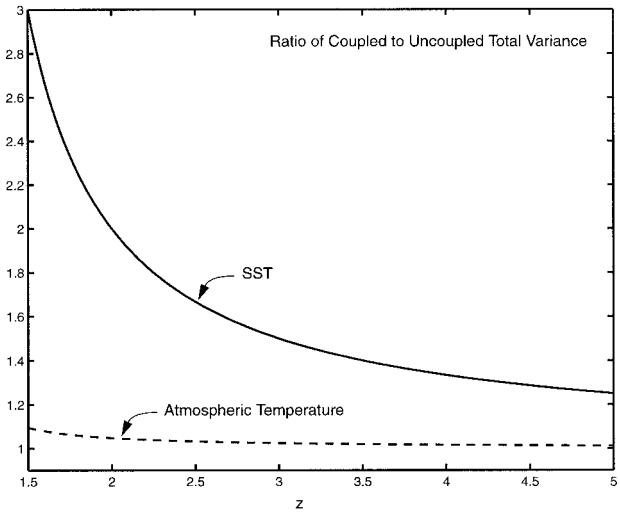

FIG. 6. Ratio of total variance between coupled and uncoupled runs for SST (solid line) and atmospheric temperature (dashed line) as a function of the stability parameter z.

atmospheric dynamical feedback (i.e., we allow only the ''thermal'' response of the atmosphere so that $b = 1$, resulting in $z = 1.25$ for the standard parameters), we get excessively large ratios between coupled and uncoupled runs. For $z < 1$, we have linearly unstable atmosphere–ocean interaction for which the stochastic model proposed here is inappropriate.

b. Integrated variance

The differing effect that coupling has on the atmosphere versus the ocean can be seen if we take the integral over all frequencies in Eqs. (14)–(19) to get the total variance. We will assume white noise forcing of unit amplitude (i.e., $|N| = 1$) to simplify the integration. The results for the uncoupled case are the simplest (see e.g., CRC Math Tables):

$$\int_0^\infty P_a^U \, d\sigma = \frac{\pi}{2a} \tag{25}$$

$$\int_0^\infty P_o^U \, d\sigma = \frac{\pi}{2\beta^2 a\tilde{d}(a + \tilde{d})}, \tag{26}$$

where $\tilde{d} = d/\beta$. For the coupled system we will show only the ratio of the total coupled power to the total uncoupled power, where we define

$$\Delta_a^{C,U} = \int_0^\infty P_a^C \, d\sigma \Big/ \int_0^\infty P_a^U \, d\sigma$$

(the corresponding ratios for oceanic variance and for the MOGA system are defined analogously). The integrals for the coupled and MOGA systems are more complicated than for the uncoupled system. The exact results are shown in appendix B. If we expand the exact results in the small parameter $\varepsilon = d/(a\beta)$, keeping only the leading order in ε, we get

$$\Delta_a^{C,U} = 1 + \frac{\varepsilon}{z - 1} + O(\varepsilon^2), \tag{27}$$

$$\Delta_o^{C,U} = \frac{z}{z - 1} \quad \text{(exact)}, \tag{28}$$

where z is as before; $\Delta_o^{C,U}$ is plotted as a function of z in Fig. 6. For the standard parameters, $\Delta_a^{C,U} = 1.03$ and $\Delta_o^{C,U} = 1.71$. The parameter ε is proportional to $\gamma_a\gamma_o^{-1}$, the ratio of the effective heat capacity of the atmosphere to that of the ocean mixed layer. Therefore, ε is inversely proportional to the mixed layer depth h. The corresponding ratios for the MOGA case are as follows:

$$\Delta_a^{M,U} = 1 + \frac{\varepsilon}{z(z - 1)} + O(\varepsilon^2) \tag{29}$$

$$\Delta_o^{M,U} = 1 + \frac{1}{(2z - 1)(z - 1)} + O(\varepsilon). \tag{30}$$

Because the bulk of atmospheric variability lies in higher frequencies where coupling has little effect, the ratio of coupled to uncoupled total atmospheric variance is near unity. On the other hand, the bulk of model oceanic variance is at low frequencies where the effect of coupling is strong, so the ocean ratio is substantially greater than 1. This reflects what happens in the two-level model of B95, as the total atmospheric variance is only slightly affected by coupling, but the oceanic variance is substantially increased by coupling (see section 4c). The effect of coupling on the total oceanic power is strictly independent of ε in the model presented here, and thus is independent of the mixed layer depth.

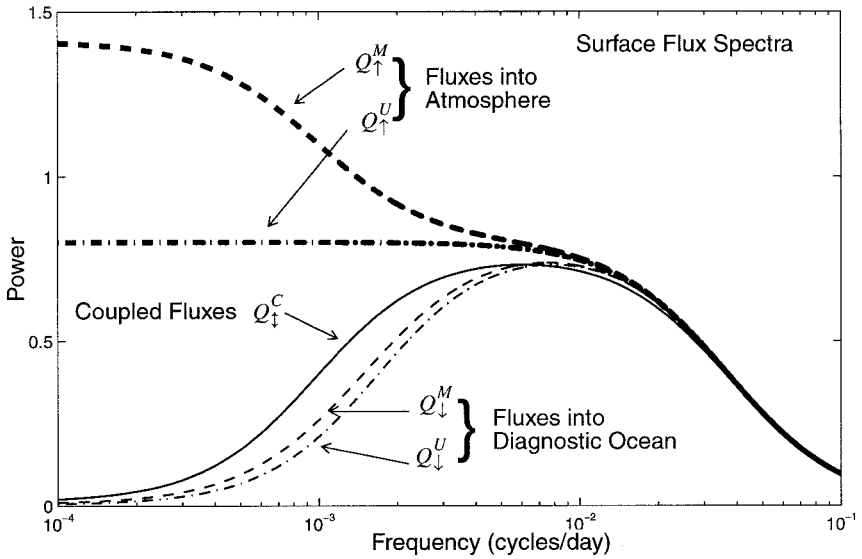

FIG. 7. Power spectra of surface flux, defined as $Q = T_s - T_o$, for coupled, MOGA, and uncoupled cases using the standard parameters. The fluxes into the atmosphere ($\uparrow$), the fluxes into the diagnostic ocean model ($\downarrow$), and the coupled fluxes ($\updownarrow$) are shown. The symbols are defined in section 3c.

c. *Surface flux spectra*

We can compute the power spectra of surface fluxes in a straightforward manner from the model equations (8)–(13), so the formulas are not shown here. For the coupled system, we define $Q^C_\updownarrow \equiv T^C_s - T^C_o = cT^C_a - T^C_o$ to be scaled symmetric surface flux. For convenience, we are neglecting the terms in the surface fluxes, that are not proportional to the air–sea temperature difference. If these terms were included, the fluxes that force the ocean would strictly go to zero for $\omega \to 0$, but otherwise the discrepancy is small. For the MOGA system, there are two sets of fluxes, those that force the atmosphere (with SSTs specified from the coupled model), $Q^M_\uparrow = T^M_s - T^C_o$, and those that force the diagnostic ocean, $Q^M_\downarrow = T^M_s - T^M_o$. Likewise, for the uncoupled system we have $Q^U_\uparrow = T^U_s$ and $Q^U_\downarrow = T^U_s - T^U_o$. These power spectra are plotted in Fig. 7. At low frequencies the fluxes that force the ocean satisfy $Q^C_\updownarrow > Q^M_\downarrow > Q^U_\downarrow$, as in B95. Given the simplicity of our ocean model, it is therefore not surprising that the resulting SST variance follows the same ordering. Also, at low frequencies $Q^U_\uparrow > Q^C_\updownarrow$. This relation is a manifestation of the reduced thermal damping in the coupled system, and it agrees with the numerical model results of B95 and Bhatt et al. (1998). Finally, $Q^M_\uparrow > Q^U_\uparrow$ at low frequencies. That is, there is a large excess of power in the low-frequency fluxes that the MOGA atmosphere sees, compared to those that the uncoupled and coupled atmospheres see. This result was somewhat unexpected in the numerical experiments of B95, particularly in light of the fact that both the atmospheric and oceanic thermal variance of the MOGA run were intermediate between the uncoupled and coupled runs. In the present model, this excess is a direct result of assuming that a large fraction of the ''natural variability'' is independent of the prescribed SST anomalies. The implications for one-way forced experiments using numerical models are discussed in section 4b.

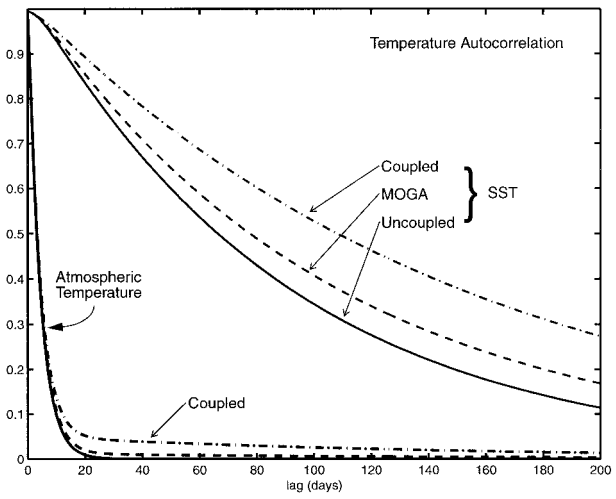

FIG. 8. Autocorrelation function for atmospheric temperature (thick lines) and SST (thin lines) for the coupled (dash–dot), MOGA (dashed), and uncoupled (solid) cases.

d. *Lag covariance*

Figure 8 shows the autocorrelation functions for T_o and T_a for the three systems with the standard parameters. The autocorrelation functions are simply the normalized Fourier transforms of the power spectra shown

in Fig. 4. Clearly, coupling significantly increases persistence of both atmospheric and oceanic temperature anomalies. Likewise, the lag covariance between T_o and T_a is the Fourier transform of $T_aT_o^*$, where the asterisk denotes the complex conjugate. The derivation of formulas for lag-covariance from Eqs. (8)–(13) is straightforward and is not shown. The lag-covariance function can then be used to derive the lag-linear regression function, which is shown in Fig. 9. Atmospheric variance, which is strongly dependent on averaging period, does not appear in the denominator of the linear regression, reducing the sensitivity of this measure to the averaging period used.

Four curves are shown in Fig. 9. The uncoupled case (curve **a**) shows strong asymmetry in lag. This asymmetry is characteristic of a system with large thermal inertia (the ocean), forced by a stochastic system with a fast decorrelation time (the atmosphere), as seen in Hasselmann (1976). The MOGA and coupled systems (curves **b** and **c**) show a progressively larger component that is symmetric in lag. The regression between the prescribed SST and the MOGA atmosphere (curve **d**) is almost entirely symmetric in lag. This symmetry is the result of the assumption that the effects of SST anomalies on the atmosphere are instantaneous. The analogous lag *correlation* functions (for pentad means) are similar in shape to those in Fig. 9, but with maximum correlations of around 0.4 for curves **a**–**c** and 0.1 for curve **d**. These curves are consistent with the lagged linear regression maps for these four cases shown in B95. For the standard parameters, the lag-correlation peaks for atmosphere leading ocean by about 10 days, a little more than twice the decorrelation time of the atmosphere.

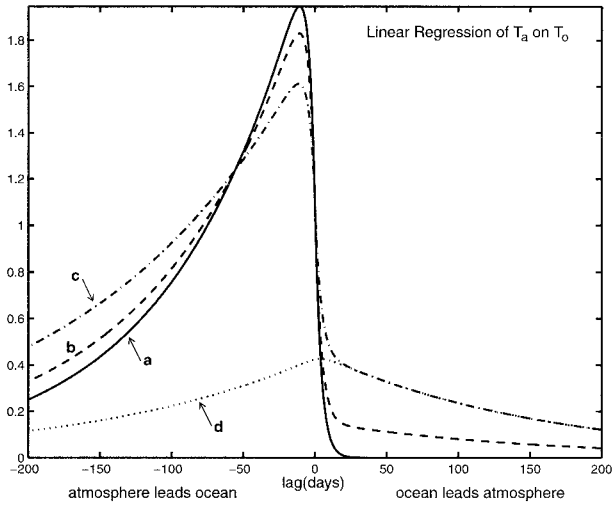

FIG. 9. Lagged linear regression between T_a and T_o. Curve **a**: T_a^U, T_o^U; curve **b**: T_a^M, T_o^M; curve **c**: T_a^C, T_o^C; curve **d**: T_a^M, T_o^C.

4. Discussion

a. General comments about coupling to slab mixed layers

To put the effects of coupling in a larger framework, consider an atmospheric GCM coupled to a slab mixed layer ocean of constant depth *h*. The value of *h* determines the nature of the lower boundary condition on the atmospheric thermodynamic equation. In the extreme case of $h \to 0$, the lower boundary condition becomes an instantaneous surface energy balance (SEB). The other extreme, $h \to \infty$, corresponds to fixed SST, where atmospheric temperature anomalies of all frequencies are damped equally by surface fluxes. The fixed SST case should exhibit the most damping due to surface fluxes, and the SEB case the least. For intermediate values of *h* the coupling acts to damp only high-frequency atmospheric temperature anomalies. For timescales longer than τ_{ML}, the SST can adjust to atmospheric temperature anomalies and the surface fluxes are reduced to near zero. As $h \to 0$, the timescale of the mixed layer becomes comparable to or shorter than the synoptic timescale in the atmosphere. Because baroclinic conversion is the ultimate source for much of midlatitude variability, the entire spectrum of variability may be affected. Therefore, we have avoided consideration of the SEB case. Instead we chose the other extreme, $h \to \infty$ (the ''uncoupled'' system, with fixed SST) as the basis for comparison with the other systems.

In the coupled and uncoupled cases, Eqs. (8)–(11), the stochastic dynamics of the atmosphere is the only source for low-frequency variability in the coupled model. In the MOGA framework however, the prescribed SST anomalies act as an additional external forcing at low frequencies [see Eqs. (12) and (13)], so we expect that the MOGA run will have more variance than the uncoupled run with its fixed, zonally symmetric SST. The question is ''How much more?'' It seems reasonable to assume, as we have done, that the bulk of the midlatitude nonlinear atmospheric variability is uncorrelated with the prescribed SST anomalies, at least for SST anomalies of modest amplitude. Evidence of this in a more realistic model is seen, for example, in the predictability study of Miller and Roads (1990), where inclusion of actual SST anomalies in midlatitudes did little to enhance predictability. Hence, it is not surprising that the MOGA atmosphere temperature variance is less than the coupled model variance. For example, Eq. (24) with the standard values for the parameters indicates that the low-frequency variance should be 1.93 times greater in the coupled framework than in the MOGA framework.

Barsugli (1995) argues that large responses to SST anomalies are not generic to atmosphere–ocean coupling, but rather depend on the special circumstances involving such factors as the climatological mean stationary waves, the position of the SST anomalies, or land–ocean temperature contrasts. Two commonly seen responses of realistic AGCMs to prescribed SST anomalies are a surface-trapped low over a warm SST anom-

aly and an equivalent barotropic high downstream from a warm SST anomaly (Palmer and Sun 1985; Peng et al. 1995). Both of these responses are consistent with the simple model presented in this paper, provided that the interaction is stable. A large barotropic response would indicate that SST anomalies couple effectively to natural barotropic variability of the atmosphere, probably through precipitation or eddy fluxes, resulting in a large effective value of *b*. Some models (e.g., Latif and Barnett 1994; Palmer and Sun 1985) show evidence of a large positive feedback; that is, $\alpha > ad$. Such a linearly unstable system is not amenable to treatment by the present stochastic model and, like any linearly unstable system, requires a mechanism for (statistical) equilibration in order to be a complete theory. The instability in the above experiments appears to arise largely because of a strong atmospheric response to SST anomalies. One would expect to see two phenomena in the presence of such strong upward coupling, which, as far as we know, are not present in the observations: First, lag–lead correlations between SST and the free atmosphere would be largely symmetric about zero lag. Second, prescription of midlatitude SST anomalies would significantly enhance predictability of the atmosphere in hindcast studies.

b. One-way forced experiments and spurious surface fluxes

In Fig. 7 we show that atmospheric models with prescribed SST can have large spurious surface fluxes at low frequencies. The largest spurious fluxes, defined as $Q_{\uparrow}^{M}/\ Q_{\updownarrow}^{C}$, occur for small values of *b* and for values of α near the stability boundary (i.e., $\alpha \approx ad$). These spurious fluxes do not present a serious problem for making short-term forecasts, as these forecast models are initialized with the correct atmospheric state from the coupled system (i.e., from observations). However, a problem may arise for seasonal predictions where SST is specified, whether specified as strict persistence of observed SST anomalies or whether these anomalies are damped back to climatology over some empirical mixed layer timescale. Specifying midlatitude SST anomalies constrains the amplitude of atmospheric temperature anomalies through the spurious (damping) surface fluxes. It would be better to make seasonal forecasts using an ensemble of runs of AGCMs coupled to mixed layer models than to use fixed boundary conditions.

The same problem arises in climate simulation studies in which the history of global SSTs is specified, or in establishing ''control run'' statistics for studies of decadal variability. The true variability in the coupled system is not necessarily well approximated by forcing the atmosphere with realistic SSTs for models with small or moderate values of the atmospheric response parameter *b*.

Numerical experiments in which atmospheric quantities are prescribed as the forcing for an ocean model suffer from a different problem. The merits of specifying surface air temperatures and winds versus specifying surface heat fluxes has been debated in the literature. Both methods suffer from problems, as both surface fluxes and air temperature are strongly coupled to the ocean temperature. If the flux forcing comes from an uncoupled or MOGA experiment, then extreme SST variance at low frequencies will result because of spurious surface fluxes. The excessive low-frequency flux forcing is often compensated by applying an arbitrary feedback term proportional to the SST anomaly. Neglecting wind-forced surface flux variance, this method is linearly equivalent to specifying surface air temperatures and winds, as long as the correct value of the feedback is chosen. This is seen in the following extension of Eq. (2):

$$\gamma_o \frac{d\tilde{T}_o}{dt} = \lambda_{so}(\tilde{T}_s - \tilde{T}_o) - \lambda_o \tilde{T}_o = \tilde{Q}_{\uparrow}^{U} - (\lambda_{so} + \lambda_o)\tilde{T}_o.$$

However, GCM boundary layer formulations usually contain a strong nonlinear dependence on the static stability of the boundary layer. Computing the forcing from atmospheric surface air temperature and wind, using a sophisticated nonlinear surface flux parametrization avoids the assumption of linearity, but the complexity of some GCM boundary layer formulations may make this an undesirable choice in practice.

The power spectrum of surface fluxes used to force a slab mixed layer model *must* tend toward zero at low frequencies, or else the temperature variance would be unacceptably large. If a more complicated ocean model is forced with spurious low-frequency fluxes, this forcing will be compensated by other oceanic processes—entrainment, advection, convection, diffusion—at these timescales. In fact, substantial low-frequency surface flux variance in a coupled model or in observations is a signature of such processes.

A potentially serious problem arises if one uses surface fluxes diagnosed from observations to force ocean models. Observational errors, which project onto all frequencies, can lead to potentially large errors in low-frequency temperature variance (e.g., Ronca and Battisti 1997). Adding a simple linear relaxation term, as discussed above, is not entirely satisfactory, as there exists some frequency below which the temperature variance is determined primarily by the error variance in the surface fluxes. In effect, random (uncorrelated in time) observational error in surface fluxes results in a low-frequency limit below which one is unable to model temperature variance reliably.

c. Comparison with more complete atmosphere and ocean models

Barsugli (1995) performed uncoupled, MOGA, and coupled integrations in which the atmosphere was modeled by the global, two-level primitive equations with parameterized convection and radiation [similar to the

TABLE 2. Enhancement of power in the simple stochastic model with the standard parameter values and in the two-level model of B95. Quantities in italics are determined using the average power for periods longer than 625 days. $\overline{\theta}$ denotes the vertical mean potential temperature in the two-level atmosphere.

Ratio (Eq. in text)	Stochastic model	Two-level GCM SST (θ)
$\delta^{C,U}$ (22)	2.91	*2.69* (*1.80*)
$\delta^{M,U}$ (23)	1.50	*2.00* (*1.38*)
$\delta^{C,M}$ (24)	1.93	*1.34* (*1.30*)
$\Delta_a^{C,U}$ (27)	1.03	1.03
$\Delta_o^{C,U}$ (28)	1.71	1.87
$\Delta_a^{M,U}$ (29)	1.01	1.01
$\Delta_o^{M,U}$ (30)	1.18	1.50
$\Delta_a^{C,M}$	1.01	1.02
$\Delta_o^{C,M}$	1.45	1.24

model of Held and Suarez (1978)]. SST was either prescribed or simulated using a 50-m slab ocean model. The model geometry was idealized to be a global ocean. The coupled stochastic model qualitatively reproduces the ratio of total variance between coupled, MOGA, and uncoupled runs in B95, as shown in Table 2. The spectra of ocean and atmosphere temperature fields and surface flux fields from B95 are reproduced in Fig. 10. These are qualitatively consistent with the results from the stochastic energy balance model, as seen in a comparison of Fig. 10a to Fig. 4, and Fig. 10b to Fig 7.

The results from the three experiments in B95 support the hypothesis for the twofold effects of coupling: the reduction of thermal damping at low frequencies and the relatively weak direct effect of forcing by SST anomalies. There are, however, two major discrepancies between the variance ratios predicted by Eqs. (22)–(24) from the stochastic coupled model and those calculated from the two-level GCM of B95. First, the low-frequency variance enhancement in the atmosphere is generally less than that of the ocean (see Table 2), and the enhancement decreases as one passes from the surface to 250 mb (not shown). Clearly, in the two-level model there can exist variability with a vertical structure that has no signature in surface temperature, and thus does not participate in coupling. This additional atmospheric variability dilutes the enhancement of variance one would expect from a univariate model such as we have presented. The second major discepancy is seen in the wavenumber-frequency spectra of B95—enhancement of variance is a strong function of zonal wavenumber. The explanation lies in the modal structure of variability in the two-level model. There are two horizontal modes that participate strongly in the coupling, a deep, equivalent barotropic mode with zonal wavenumber $k = 4$, and a shallow $k = 1$ mode. The former is the dominant mode of low-frequency variability in the uncoupled case and is merely enhanced by the coupling to the mixed layer. The latter appears strongly in the coupled run but only very weakly in the uncoupled run, and can be explained as a surface-trapped advective, coupled mode (Frankignoul 1985; B95). The $k = 1$ mode also appears

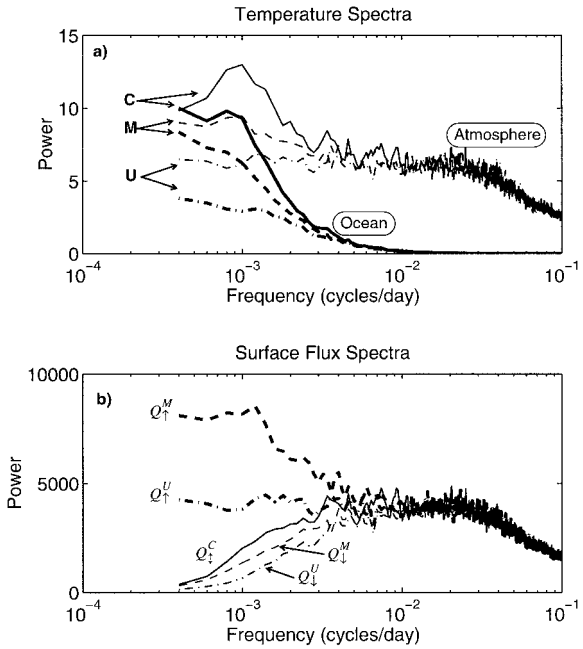

FIG. 10. (a) As in Fig. 4 but for power spectra of SST and atmospheric vertical mean potential temperature from integrations of the two-level model of B95. (b) As in Fig. 7 but for power spectra of total surface fluxes from the two-level model.

strongly in the MOGA run spectrum, suggesting a large value of α associated with this mode. These discrepancies, and the associated dynamical reasons for them, are indicative of what to expect from the analysis of more realistic models.

Manabe and Stouffer (1996) present results from the GFDL R15 AGCM in which the AGCM was (i) integrated using the prescribed annual cycle of SST and (ii) coupled to a 50-m slab mixed layer, and (iii) coupled to an ocean GCM. They found that coupling acted to enhance the variance of SST and surface air temperature in the midlatitudes, with the greatest increase occurring at lowest frequencies (see their Figs. 1–5). In Fig. 1 we have reproduced their Fig. 4b, showing the ratio of standard deviations between their coupled GCM and fixed SST runs. The coarse contour interval in their figures makes it difficult to determine quantitatively the extent of the agreement between their GCM and the stochastic model. However, their figures indicate that the ratio of coupled-to-uncoupled variance (derived by squaring their standard deviations) in surface air temperature in midlatitudes is roughly 2.5 for 5-yr averaged fields, whereas the stochastic model yields a ratio between 2.4 (period 5 yr) and 2.9 (period infinity). Significantly, the ratios of variance between the models with the ocean GCM and the slab mixed layer are near unity over much of the open oceans (their Fig. 4a). Furthermore, the GFDL coupled AGCM/OCGM yields midlatitude spectra of surface air temperature and SST (their Fig. 12) that are remarkably similar in structure to that from the

simple stochastic model. However, the GFDL model yields slightly more variance in SST than in surface air temperature (unlike the stochastic model) for periods greater than about 20 years, presumably due to variability associated with changes in the oceanic thermohaline circulation.

Bladé (1997) used the same atmosphere GCM as in Manabe and Stouffer (1996) to examine the effect of midlatitude coupling on the variability in the midlatitude atmosphere. In this study, the control integration was compared to an integration in which the atmosphere was coupled to a 50-m slab ocean in the midlatitudes of both hemispheres; both integrations featured perpetual January solar forcing. Bladé reported that the influence of midlatitude coupling significantly enhanced the midlatitude lower tropospheric temperature and circulation variance at the lowest frequencies. For example, the ratio of coupled-to-uncoupled power in the 850-mb air temperature over the midlatitude oceans at lowest frequencies is approximately 1.6. Bladé (1997) furthermore noted that the effect of midlatitude coupling in the full GFDL GCM was quantitatively similar to that found in the idealized two-level GCM studies of B95.

Bhatt et al. (1998) examined the differences in the atmospheric circulation anomalies that result from coupling the NCAR CCM1 R15 AGCM to the variable-depth mixed layer model of the North Atlantic Ocean. Both coupled and control integrations were 35 yr long and include a seasonal cycle. Compared to the control integration, the variance of the wintertime averaged surface air temperature in the coupled integration increased by a factor of about 2.3. The net surface heat fluxes decreased by a factor of about 0.6. Coupling also enhanced the persistence of the principal mode of variability in the atmosphere. These results are in agreement with predictions from the stochastic model.

While the simple model we present was developed to explain enhancement of internally generated midlatitude low-frequency variability, it is also applicable to externally forced variability. Lau and Nath (1996) reported the results from a series of experiments with the GFDL R15 AGCM on the effect of midlatitude coupling on tropically forced midlatitude variability. In these experiments they examined the portion of the midlatitude variability in the ocean and atmosphere that is associated with ENSO via atmospheric teleconnections (''the atmospheric bridge'') by prescribing observed tropical Pacific SST anomalies under the AGCM. The effect of the coupling in the midlatitudes on the ENSO-forced midlatitude variability was determined by examining differences between two ensembles of integrations: the first ensemble held midlatitude SST fixed at climatological values (TOGA), while the second ensemble allowed the midlatitude atmosphere to interact with a 50-m slab ocean (TOGA-ML). The principal results of Lau and Nath's study are qualitatively consistent with the stochastic model results. Specifically, the ENSO-related variance in the surface air temperature over the North Pacific Ocean, which is predominantly at low frequencies, increased about fourfold due to coupling.[3] The variance and persistence of the 500-mb and surface atmospheric circulation anomalies associated with the ENSO were also enhanced by the midlatitude atmosphere–ocean coupling, consistent with the enhancement in the temperature variance via the thermal-wind relation. The structure of the midlatitude ENSO-related anomalies was found to be insensitive to midlatitude coupling.

In a similar investigation to Lau and Nath (1996), Alexander (1992) concluded that ''air–sea interaction primarily acts to damp ocean anomalies,'' whereas we come to the opposite conclusion. The resolution of this seeming contradiction is that he compared his coupled SSTs to SSTs from an ocean model forced by surface fluxes from his uncoupled atmosphere integrations ($dT_o/dt = Q_\uparrow^U$ in our notation). As discussed in section 3c, this latter methodology produces spuriously large SST variability, and does not serve to illuminate the basic role of coupling. In fact, what Alexander (1992) calls ''partially coupled'' SST is equivalent to our ''uncoupled SST,'' and indeed shows about half the temperature signal compared to his coupled SST away from the continents in winter, thus confirming our viewpoint.

d. Caveat concerning the use of this model to interpret GCM results

The main virtues of the model in Eqs. (8)–(13) are its simplicity and flexibility. One is tempted to use it to quantitatively diagnose output from atmospheric GCMs coupled to slab mixed layer oceans. *Caveat emptor*: the model as it stands is oversimplified in several important aspects, making it unsuitable to use for quantitative diagnosis. We believe that the major oversimplifications are as follows: the assumption of a first-order Markov process for an uncoupled atmosphere model, the assumption of purely thermal coupling, and the neglect of modal structure in the atmosphere. We will discuss these below.

The uncoupled atmosphere model of Eq. (10) does not generally capture the spectrum of low-frequency variability in more realistic GCMs. However, the exact form taken by the uncoupled atmosphere equation is not critical to understanding the basic effects of atmosphere–ocean coupling. For example, the 850-mb temperature power spectrum from and uncoupled run of the GFDL R15 AGCM (Bladé 1997), taken at grid points over the North Pacific Ocean, cannot be fit by Eq. (10). However, an ad hoc fit to the GCM spectrum may be obtained using Eq. (10) with an 8-day damping time-

[3] This enhancement was estimated by comparing the squares of the linear regression coefficients at the ''bull's-eye'' in the North Pacific (Figs. 3c and 12c of Lau and Nath) for the TOGA and TOGA-ML runs.

scale, assuming that there is an additional background white noise variance. The qualitative results of this paper still hold in this case, and the quantitative calculations may be carried through with only slight modifications.

While purely thermal effects seem to explain much of the phenomenology of atmosphere–ocean coupling in realistic GCM experiments, it is not the whole story, even if the ocean is a slab mixed layer. Low-frequency surface wind variability and nonlinear moisture variability may modulate surface fluxes independent of the air–sea temperature difference. If these effects play a significant role, then the surface temperature (and moisture) variability will differ substantially from SST variability at low frequencies. Wind variability also drives Ekman currents in the ocean, which we have neglected. These effects are discussed in Liu (1993) and Miller (1992) and provide a complementary approach to ours.

Finally, atmospheric variability has vertical and horizontal structure. A single variable is at best a crude representation of what is inherently a multivariate system. It is tempting to interpret the single atmospheric temperature variable in Eqs. (8)–(13) as representing a single mode of atmospheric variability. Indeed we have done so in this paper in interpreting the results of B95. However, it must be kept in mind that the total variability (say, at a grid point) may be the amalgam of modes with widely differing behavior under coupling. In addition, atmosphere–ocean coupling may allow for interaction between ''uncoupled'' atmospheric modes through diabatic or nonlinear heating anomalies associated with SST anomalies.

5. Conclusions

The primary purpose of this simple stochastic model is heuristic: to interpret the results from more realistic models in a simple framework. The stochastic model can be interpreted as representing the variability at a characteristic location in midlatitudes, or as representing a dominant mode of midlatitude variability. The physical mechanism that this model presents is that coupling between atmosphere and ocean reduces the internal damping of temperature anomalies due to surface heat fluxes. Reduced damping in the presence of a constant level of stochastic forcing in the atmosphere leads to greater thermal variance of the coupled atmosphere and ocean compared to the uncoupled atmosphere and to the uncoupled ''slave'' ocean. The MOGA (specified SST) model is generally unable to reproduce the coupled model variance because of the stochastic (unpredictable) component of the midlatitude circulation. These results have major implications for midlatitude predictability studies and for the interpretation of AMIP runs (see section 4b).

We have introduced an atmospheric response parameter that roughly characterizes the atmospheric response to SST anomalies. We have assumed that free atmosphere variability is linked to surface air temperature variability by a proportionality constant. These two effects combine to form the coupling coefficient α. Despite the great simplification involved in reducing the atmospheric dynamics to one parameter, this parameter can be an extremely useful tool to characterize the coupled system. For example, the stochastic model demonstrates the strong sensitivity of the midlatitude coupled system to the strength of coupling.

The results from the simple stochastic model are consistent with the results from several studies using more realistic coupled models. The enhancement of variance due to coupling in fully coupled atmosphere–ocean GCMs is generally of the magnitude predicted by the stochastic model. This suggests that most of the effect of coupling between the midlatitude atmosphere and ocean is the result of reduced thermal damping. Our simple model is restricted to purely thermal coupling between the atmosphere and ocean, omitting many physical processes. Nevertheless, these thermal effects alone are able to capture the basic effects of coupling, even in models with active ocean dynamics such as Manabe and Stouffer (1996). Perhaps the most significant omission in the simple stochastic model is that of the mechanically driven Ekman currents in the ocean, at least for understanding seasonal to interannual variability.

The simple model presented here provides a conceptual model for understanding the overall effects of coupling between the atmosphere and the ocean in midlatitudes. It also suggests that the experimental design of an atmospheric model coupled to a mixed layer ocean model (likely more sophisticated than a slab model) would provide a reasonable null hypothesis against which to test for the presence of distinctive decadal variability. In addition, it is hoped that this model, or refinements of it, will be applied to the quantitative diagnosis of more realistic GCM runs and of the observational record.

Acknowledgments. A preliminary version of this work was done as part of JJB's Ph.D. dissertation at the University of Washington under the supervision of Dennis Hartmann. We are grateful for conversations with Ileana Bladé, Mike Wallace, Art Miller, and Prashant Sardeshmukh during the course of bringing this work to publication. We also thank Paul Schopf for bringing to our attention his earlier work with a similar model. JJB was supported by NSF Grant ATM-9313383 at the University of Washington and by a grant from the NOAA Office of Global Programs; DSB was supported by grants from the NOAA Office of Global Programs, through the Atlantic Climate Change Program and the Hayes Center.

This publication is partially funded by the Joint Institute for the Study of the Atmosphere and Ocean under NOAA Cooperative Agreement NA67RJ0155. The views expressed herein are those of the author(s) and

do not necessarily reflect the views of NOAA or any of its subagencies.

APPENDIX A

Derivation of the Energy Balance Model

This derivation will provide a more detailed physical interpretation of Eqs. (1) and (2), and will guide us in estimating reasonable values for the free parameters not discussed in the main text, namely λ_a, λ_o, λ_{sa}, and λ_{so}. The original motivation for the heuristic model Eqs. (1) and (2) was to explain the results of Barsugli (1995), who used a two-level atmospheric model with simplified physics. Hence, the assumptions used here are guided by the formulation and behavior of that model. In this appendix we will adopt the view that the stochastic model is relevant to the vertically averaged equations of the real atmosphere. (In the main text we discussed an alternate interpretation of the stochastic model as representing modes of atmosphere–ocean variability).

We treat the atmosphere as a single graybody layer with effective temperature T_a, longwave emissivity $\varepsilon_a = 0.76$, and heat capacity γ_a. The ocean is treated as a well-mixed layer with heat capacity γ_o. The resulting balance between shortwave, longwave, surface, and dynamical fluxes is shown in Fig. 2, where the variables are defined. The equations are as follows (all variables in this appendix are in physical space, so we have dropped the tildes used in the main text):

$$\gamma_a \frac{\partial T_a}{\partial t} = R_a + \varepsilon_a \sigma_B T_o^4 - 2\varepsilon_a \sigma_B T_a^4 + \lambda(T_o - T_s) + \mathcal{F}, \quad \text{(A1)}$$

$$\gamma_o \frac{\partial T_o}{\partial t} = R_o - \sigma_B T_o^4 + \varepsilon_a \sigma_B T_a^4 - \lambda(T_o - T_s), \quad \text{(A2)}$$

where σ_B is the Stefan–Boltzman constant, $\mathcal{F}$ represents the dynamical forcing of the atmosphere, and R is the shortwave radiative heating. The combined surface turbulent latent and sensible heat fluxes are linearized, and λ, the proportionality constant between these fluxes and the air–sea temperature difference, is assumed to be constant. Latent heat is also assumed to be released locally. To close the system we assume $T_s = cT_a$. If we assume a constant atmospheric lapse rate and a constant effective longwave emission height, then $c = 1$. This assumption is suggested by the observation that at very low frequencies, temperature anomalies display a strongly barotropic vertical structure in the troposphere. This latter assumption is almost certainly an oversimplification.

We are interested only in the perturbations about the climatology (denoted by ''primed'' variables), so the steady solution will not be shown. We construct perturbation equations by linearizing about the steady solution to Eqs. (A1) and (A2), denoted by $\overline{T}_a$ and $\overline{T}_o$. We also regroup terms so that the contribution by T_o' to the longwave flux in the atmosphere equation is included entirely in the term proportional to the air–sea difference (likewise for the T_a' contribution to the ocean equation):

$$\gamma_a \frac{\partial T_a'}{\partial t} = R_a' + (\lambda + 4\varepsilon_a \sigma_B \overline{T}_o^3)(T_o' - T_s') - 4\varepsilon_a \sigma_B (2\overline{T}_a^3 - \overline{T}_o^3) T_a' + \mathcal{F}' \quad \text{(A3)}$$

$$\gamma_o \frac{\partial T_o'}{\partial t} = R_o' - (\lambda + 4\varepsilon_a \sigma_B \overline{T}_a^3)(T_o' - T_s') - 4\sigma_B (\overline{T}_o^3 - \varepsilon_a \overline{T}_a^3) T_o'. \quad \text{(A4)}$$

Note that Eqs. (A3) and (A4) are in the same form as Eqs. (1) and (2), provided that we assume $R_a' = R_o' = 0$. (This is an extremely good approximation in the two-level model of B95, less so in more realistic GCMs.)

The parameters in Eqs. (1) and (2) may now be estimated. The surface flux proportionality constant, λ, can be estimated from the linear regression of the sum of sensible and latent fluxes versus the ocean–atmosphere temperature difference. Estimates from the two-level model of B95 for λ as a function of latitude yield $\lambda = 20$ W m^{-2} K^{-1} as a representative midlatitude value. If we choose $\overline{T}_a = 270$ K, and $\overline{T}_o = 285$ K, we have (in units of W m^{-2} K^{-1}) $\lambda_{sa} = 23.9$, $\lambda_{so} = 23.4$, $\lambda_a = 2.8$, and $\lambda_o = 1.9$. For the standard parameter values, we also assume $b = 0.5$ (discussed in the text), $c = 1$, and N to be white noise forcing of unit amplitude. The standard parameter values are summarized in Table 1. The ocean and atmosphere heat capacities listed in Table 1 are for a 50-m slab of water and for a 1000-mb deep column of air, respectively.

Finally we would like to be more explicit about our treatment of the atmospheric dynamics. The simplest possible parameterization of atmospheric dynamics that retains both the deterministic and random components of the dynamics is

$$\mathcal{F} = -\lambda_d T_a + M. \quad \text{(A5)}$$

The term $\lambda_d T_a$ is the univariate representation of the bulk effects of the deterministic dynamics of the atmosphere and includes the linearly parameterizable effects of the transient eddies. The stochastic forcing term M represents the purely random, unpredictable effects of the transient eddies. We can obtain a better approximation to the coupled system by extending the parameterization to allow for the linear effects of SST anomalies as follows:

$$\mathcal{F} = -\lambda_d T_a + \lambda_d' T_o + M, \quad \text{(A6)}$$

where the stochastic forcing is now assumed to be independent of the coupling. Because the purely dynamical feedback cannot presently be estimated from first principles, we have chosen to neglect this effect. In obtaining Eqs. (6) and (7), we have used Eq. (A6) with $\lambda_d = 0$, $N = M/\lambda_{sa}$, and $b = \lambda_d'/\lambda_{sa} + 1$. We have also

neglected cloud radiative feedback. These missing feedbacks could be estimated on a model-by-model basis from GCM output, and they are likely candidates for explaining the discrepancy between the atmospheric timescale of the simple model with the ''standard parameters'' and the timescale estimated from GCMs.

APPENDIX B

Evaluation of the Total Variance Integrals

The indefinite integrals of the quantities in Eqs. (25)–(30) could be performed via a partial fraction decomposition. This procedure would allow us to prescribe some upper cutoff in our integration at high frequencies. However, if one is willing to approximate the total variance by integrating over all frequencies from $0 \rightarrow \infty$, then it is simpler to consider these definite integrals as being in the complex plane and to evaluate them by summing over the residues at the poles of the integrand in the upper half-plane, the procedure we sketch here. The polynomial

$$\sigma^4 + (A^2 - 2B)\sigma^2 + B^2, \tag{B1}$$

where $A = a + d/\beta$, and $B = (ad + \alpha)/\beta$ appears in the denominator of several of the integrals. For the solutions presented here to be valid, the roots of Eq. (B1) must not lie on the real axis. This requires $a - d/\beta > 4\alpha/\beta$, which is easily satisfied for the standard parameters. This allows us to write Eq. (B1) as $(\sigma^2 + r_1^2)(\sigma^2 + r_2^2)$. Special properties of the roots, $r_1 + r_2 = A$ and $r_1 r_2 = B$, are used in obtaining the following, exact results for the coupled and MOGA systems (the exact uncoupled results were presented in the text):

$$\int_0^\infty P_a^C \, d\sigma = \frac{\pi}{2(a + \tilde{d})}\left[1 + \frac{\tilde{d}}{a}\frac{z}{z - 1}\right] \tag{B2}$$

$$\int_0^\infty P_o^C \, d\sigma = \frac{\pi}{2\beta^2 a\tilde{d}(a + \tilde{d})}\left[\frac{z}{z - 1}\right] \tag{B3}$$

$$\int_0^\infty P_a^M \, d\sigma = \frac{\pi}{2a}\left[1 + \frac{2a + \tilde{d}}{(a + \tilde{d})(z - 1)\left(2a^2\dfrac{\beta}{\alpha} + 2z - 1\right)}\right] \tag{B4}$$

$$\int_0^\infty P_o^M \, d\sigma = \frac{\pi}{2\beta^2 a\tilde{d}(a + \tilde{d})}\left[1 + \frac{R}{z - 1}\right] \tag{B5}$$

where

$$R = \frac{W + 2z - 1}{W(2z - 1) + 1}$$

and

$$W = \frac{2(a + \tilde{d})}{\tilde{\alpha}}, \qquad \tilde{d} = \frac{d}{\beta}, \qquad \tilde{\alpha} = \frac{\alpha}{\beta}.$$

REFERENCES

Alexander, M. A., 1992: Midlatitude air–sea interaction during El Niño. Part I: The North Pacific Ocean. *J. Climate,* **5,** 944–958.

Barsugli, J. J., 1995: Idealized models of intrinsic midlatitude atmosphere–ocean interaction. Ph.D. dissertation, University of Washington, 189 pp.

Bhatt, U. S., M. A. Alexander, D. S. Battisti, D. D. Houghton, and L. A. Keller, 1998. Atmosphere–ocean interaction in the North Atlantic: Near surface climate variability. *J. Climate,* in press.

Bladé, I., 1997: The influence of midlatitude ocean–atmosphere coupling on the low-frequency variability of a GCM. Part I: No tropical SST forcing. *J. Climate,* **10,** 2087–2106.

Frankignoul, C., 1985: Sea surface temperature anomalies, planetary waves, and air–sea feedback in the middle latitudes. *Rev. Geophys.,* **23,** 357–390.

——, and K. Hasselmann, 1977: Stochastic climate models. Part II: Application to sea-surface temperature anomalies and thermocline variability. *Tellus,* **29,** 284–305.

——, and R. W. Reynolds, 1983: Testing a dynamical model for midlatitude sea surface temperature anomalies. *J. Phys. Oceanogr.,* **13,** 1131–1145.

Gates, W. L., 1992: AMIP: The Atmospheric Model Intercomparison Project. *Bull. Amer. Meteor. Soc.,* **73,** 1962–1970.

Hasselmann, K., 1976: Stochastic climate models. I, Theory. *Tellus,* **28,** 473–485.

Held, I. M., and M. J. Suarez, 1978: A two-level primitive equation atmospheric model designed for climatic sensitivity experiments. *J. Atmos. Sci.,* **35,** 206–229.

Kim, K.-Y., and G. R. North, 1992: Seasonal cycle and second-moment statistics of a simple coupled climate system. *J. Geophys. Res.,* **97,** 10 069–10 081.

Latif, M., and T. P. Barnett, 1996: Decadal climate variability over the North Pacific and North America: Dynamics and predictability. *J. Climate,* **9,** 2407–2423.

Lau, N.-C., and M. J. Nath, 1994: A modeling study of the relative roles of tropical and extratropical SST anomalies in the variability of the global atmosphere–ocean system. *J. Climate,* **7,** 1184–1207.

——, and ——, 1996: The role of the ''atmospheric bridge'' in linking tropical Pacific ENSO events to extratropical SST anomalies. *J. Climate,* **9,** 2036–2057.

Liu, Z., 1993: Interannual positive feedbacks in a simple extratropical air–sea coupling system. *J. Atmos. Sci.,* **50,** 3022–3028.

Manabe, S., and R. J. Stouffer, 1996: Low-frequency variability of surface air temperature in a 1000-yr integration of a coupled ocean–atmosphere model. *J. Climate,* **9,** 376–393.

Marotzke, J., and D. W. Reynolds, 1997: On spatial scales and lifetimes of SST anomalies beneath a diffusive atmosphere. *J. Phys. Oceanogr.,* **27,** 133–139.

Miller, A. J., 1992: Large-scale ocean–atmosphere interactions in a simplified coupled model of the midlatitude wintertime circulation. *J. Atmos. Sci.,* **49,** 273–286.

——, and J. O. Roads, 1990: A simplified coupled model of extended-range predictability. *J. Climate,* **3,** 523–542.

Nitsche, G., 1996: Some aspects of planetary-scale atmospheric variability in a low-resolution general circulation model. Ph.D. dissertation, University of Washington, 207 pp.

North, G. F., and R. F. Cahalan, 1981: Predictability in a solvable stochastic climate model. *J. Atmos. Sci.,* **38,** 504–513.

——, J. Mengel, and D. Short, 1983: Simple energy balance model resolving the seasons and the continents: Application to the astronomical theory of the ice ages. *J. Geophys. Res.,* **88,** 6576–6586.

Palmer, T. N., and Z. Sun, 1985: A modeling and observational study of the relationship between sea surface temperatures in the northwest Atlantic and the atmospheric general circulation. *Quart. J. Roy. Meteor. Soc.,* **111,** 947–975.

Peng, S., L. A. Mysak, H. Ritchie, J. Derome, and B. Dugas, 1995: The differences between early and midwinter atmospheric responses to sea surface temperature anomalies in the northwest Atlantic. *J. Climate,* **8,** 137–157.

Ronca, R. E., and D. S. Battisti, 1997: Anomalous sea surface temperatures and local air–sea energy exchange on intraannual timescales in the northeastern subtropical Pacific. *J. Climate,* **10,** 102–117.

Schneider, E. K., and J. L. Kinter III, 1994: An examination of internally generated variability in long climate simulations. *Climate Dyn.,* **10,** 181–204.

Schopf, P. S., 1985: Modeling tropical sea-surface temperature: Implications of various atmospheric responses. *Coupled Ocean-Atmosphere Models,* J. C. J. Nihoul, Ed., Elsevier, 727–734.

Zubarev, A. P., and P. F. Demchenko, 1992: Predictability of the averaged global air temperature in a simple stochastic atmosphere–ocean interaction model. *Izv. Atmos. Oceanic Phys.,* **28,** 19–23.